THE JOURNAL OF BIOLOGICAL CHEMISTRY VOL. 284, NO. 13, pp. 8661–8669, March 27, 2009

Defining the Potassium Binding Region in an Apple Terpene Synthase*[S]

Received for publication, September 15, 2008, and in revised form, January 29, 2009 Published, JBC Papers in Press, January 29, 2009, DOI 10.1074/jbc.M807140200

Sol Green[‡§1], **Christopher J. Squire**[§], **Niels J. Nieuwenhuizen**[‡], **Edward N. Baker**[§], **and William Laing**[‡]

From [‡]*The New Zealand Institute for Plant and Food Research, Mt. Albert, Private Bag 92169, Auckland and the* [§]*School of Biological Sciences and Centre of Molecular Biodiscovery, University of Auckland, Private Bag 92019, Auckland, New Zealand*

Terpene synthases are a family of enzymes largely responsible for synthesizing the vast array of terpenoid compounds known to exist in nature. Formation of terpenoids from their respective 10-, 15-, or 20-carbon atom prenyl diphosphate precursors is initiated by divalent (M^{2+}) metal ion-assisted electrophilic attack. In addition to M^{2+}, monovalent cations (M^+) have also been shown to be essential for the activity of certain terpene synthases most likely by facilitating substrate binding or catalysis. An apple α-farnesene synthase (MdAFS1), which has a dependence upon potassium (K^+), was used to identify active site regions that may be important for M^+ binding. Protein homology modeling revealed a surface-exposed loop (H-αl loop) in MdAFS1 that fulfilled the necessary requirements for a K^+ binding region. Site-directed mutagenesis analysis of specific residues within this loop then revealed their crucial importance to this K^+ response and strongly implicated specific residues in direct K^+ binding. The role of the H-αl loop in terpene synthase K^+ coordination was confirmed in a Conifer pinene synthase also using site-directed mutagenesis. These findings provide the first direct evidence for a specific M^+ binding region in two functionally and phylogenetically divergent terpene synthases. They also provide a basis for understanding K^+ activation in other terpene synthases and establish a new role for the H-αl loop region in terpene synthase catalysis.

Terpenoids comprise the largest and most diverse class of natural products known (1). Terpenoid structures range from simple acyclic molecules to complex heterocyclic ring systems. These compounds are synthesized by a large family of enzymes called terpene synthases (TPS).[2] In plants, monoterpenes (C10-based) are synthesized from the plastid-derived geranyl diphosphate (GDP), sesquiterpenes (C15-based) from the cytoplasmically derived farnesyl diphosphate (FDP) and diterpenes (C20-based) from geranylgeranyl diphosphate, which is also plastid-derived. Although these compounds provide biosynthetic building blocks to various primary metabolites including hormones and photosynthetic pigments, the majority function as secondary metabolites. These improve the ecological fitness of the organism by enabling communication to pollinators and seed dispersal agents and the provision for defense against pathogens and herbivores (2–5). Terpenes can also affect quality traits, including susceptibility to storage disorders, in crops such as apples (6) and pears (7).

Divergent TPS share various structural features. These include a highly conserved C-terminal domain, which contains their catalytic site (8) and an aspartate-rich DD*XX*D motif (9) essential for the divalent metal ion (typically Mg^{2+} or Mn^{2+}) assisted substrate binding in these enzymes (10–14). This conservation is also shared in their reaction chemistry, which is characterized by electrophilically initiated carbocation formation, carbocation stabilization, and rearrangement, incorporating exquisite regio- and stereospecificity, to generate structurally diverse products (15–17).

Numerous enzymes in plants and animals are now known to be activated by monovalent cations (M^+) (18, 19). The role of M^+ cations in enzyme activation is to facilitate substrate binding by lowering energy barriers in the ground and/or transition states rather than being the causative agents of catalysis (20). The inability of M^+ to direct catalysis, unlike divalent metal ions (*e.g.* M^{2+} in TPS), results from insufficient charge density, due to the spread of a single charge over a large volume (20). The tight *in vivo* regulation of M^+ levels (20) also means that the enzyme active site would always be charged with M^+, and M^+ would not be a physiologically relevant regulator of enzyme activity. MdAFS1 has a specific dependence on K^+ for normal function, and has a reported affinity constant (K_a) of ~3 mM for K^+ (21). Although this is higher than the reported k_a of ~0.7 mM for Mg^{2+}, it is well below the generally accepted 100–200 mM K^+ concentration known to exist in plants (22).

Crystal structure analyses have established that the M^+ acts either in a cofactor-like or an allosteric-like manner (20). Enzymes exhibiting the cofactor-like response are cat-

* This work was supported by New Zealand Foundation for Research, Science, and Technology Grant C06X0403 and Plant & Food Internal Investment funding. The costs of publication of this article were defrayed in part by the payment of page charges. This article must therefore be hereby marked "*advertisement*" in accordance with 18 U.S.C. Section 1734 solely to indicate this fact.

[S] The on-line version of this article (available at http://www.jbc.org) contains supplemental Figs. S1–S5 and Tables S1 and S2.

[1] To whom correspondence should be addressed: Plant & Food Research, Mt. Albert Research Centre, 120 Mt. Albert Rd., Private Bag 92169, Auckland, New Zealand. Tel.: 64-9-815-4200; Fax: 64-9-9258628; E-mail: sol.green@hortresearch.co.nz.

[2] The abbreviations used are: TPS, terpene synthase; GDP, geranyl diphosphate; FDP, farnesyl diphosphate; MdAFS1, *Malus x domestica* α-farnesene synthase; Bistris propane, 1,3-bis[tris(hydroxymethyl)methylamino]propane; WT, wild type; GC-MS, gas chromatography-mass spectrometry; BPPS, bornyldiphosphate synthase.

egorized as type I. They are absolutely dependent upon M^+, which is required either for substrate binding (type Ia) or substrate hydrolysis (type Ib). Enzymes exhibiting the allosteric-like response are categorized as type II. Although their activity is not absolutely dependent upon M^+, it is enhanced through conformational changes triggered by M^+ binding to a site that does not involve direct contact with substrate. M^+ binding in enzymes also often occurs in tandem with that of a divalent cation such as Mg^{2+} (20). The dependence of TPS upon M^+ (specifically K^+) was first identified in conifer mono-TPS (23), and more recently in an apple sesqui-TPS (21). Mechanistically, however, TPS reactions, which are initiated by electrophilic assistance to the C-O cleavage of diphosphate esters (15, 16, 24–30), contrast with other M^+-dependent enzymes. These latter enzymes are predominantly associated with phosphoryl transfer reactions (18, 19), and catalyze the P-O bond cleavage of phosphate esters via nucleophilic displacement.

A number of TPS crystal structures have been solved (8, 31–36). There are, however, no structures available for a K^+-dependent enzyme, and hence there are no reports specifically indicating which groups may be important for binding. In this paper, we investigate the K^+ binding region in an apple (*Malus x domestica*) α-farnesene synthase (MdAFS1) (21, 37). To investigate how and where K^+ is bound in MdAFS1 we use a homology modeling approach to predict groups that may be involved. We then use site-directed mutagenesis to modify those groups and determine their importance. Site-directed mutagenesis was also used to establish the importance of this loop in the activity of other TPS.

EXPERIMENTAL PROCEDURES

Sequence Analysis—Multiple amino acid sequence alignments of TPS were performed with ClustalX (38), using default parameters, and were manually adjusted in GeneDoc (nrbsc.org/gfx/genedoc/). Evolutionary relationships in the TPS-b synthases were inferred using the Neighbor-Joining method (39). The evolutionary distances were computed using the Poisson correction method (40). Phylogenetic analyses were conducted in MEGA4 (41).

Molecular Modeling—A homology model for MdAFS1 was constructed using Modeler9 version 1 (42), using the x-ray crystal structures of bornyldiphosphate synthase from *Salvia officinalis* (Protein Data Bank codes 1N1Z and 1N1B) (36) as a template. After sequence alignment and docking onto the template structure, side chains in the active site region were adjusted manually and hydrated Mg^{2+} cations were placed in similar locations as in PDB codes 1N1Z and 1N1B. Hydrogen atoms were added to the structure, charges were assigned (Gasteiger method), and the model was energy-minimized in Sybyl7.2 (www.tripos.com/sybyl). An FDP substrate molecule was built, charges assigned and minimized in Sybyl before being docked into the protein model using the program GOLD (43). The docking was deliberately biased using a template-similarity constraint to position the diphosphate moiety in a similar manner to that observed in TPS crystal structures, bound to the Mg^{2+} in an appropriate geometry. The active site cavity was automatically detected by GOLD, by searching a 10-Å radius space around Asp^{453}. Multiple GOLD solutions consistently placed the substrate molecule in the same site, with the diphosphate bound to the Mg^{2+} ions. Of 10 models examined, all exhibited extended FDP conformations deep into the active site, with four solutions clustered closely around the top solution, as predicted by Goldscore. Images were formulated in PyMol (DeLano Scientific: pymol.sourceforge.net).

Mutagenesis of Terpene Synthase Genes—Mutated enzymes were generated using the QuikChange II™ site-directed mutagenesis kit (Stratagene, La Jolla, CA) according to the manufacturer's instructions. The PCR-based mutagenesis protocol was performed using pET-30a (Novagen), pET200/D-TOPO (Invitrogen) or pET101/D-TOPO (Invitrogen) harboring the respective MdAFS1 (21), AcTPS2, and pseudomature PsTPS2 (44) cDNAs as template. Mutant genes were fully sequenced to ensure fidelity. Mutagenic primers are listed in supplemental Table S1.

Production of Recombinant Proteins—The WT and mutated PsTPS2 were re-amplified from the original pET101/D-TOPO vectors and recloned into the pET200/D-TOPO vector using identical forward and reverse primers to McKay *et al.* (44). This was carried out to enable the purification and analysis of N-terminal His-tagged PsTPS2 proteins rather than using non-purified cleared bacterial lysates as previously described (44). Recombinant proteins were expressed from the above plasmids following transformation into BL21-CodonPlus™-RIL cells. Cultures (500 ml) were grown in ZYM-5052 autoinducible media (45) at 16 °C for 48–72 h at 300 rpm. Recombinant MdAFS1, PsTPS2, and AcTPS2 proteins were extracted and purified according to previous methods (21). Eluted recombinant proteins were analyzed by SDS-PAGE and terpene synthase activity measured. Protein concentrations were determined by Qbit™ analysis and microfluidic protein chips analyzed on the Experion™ automated electrophoresis system (Bio-Rad) according to the manufacturer's specifications.

FDP Activity Assays—Assays (50 μl) based on previous methods (46) were conducted in quadruplicate, and typically contained 300 nM recombinant protein in assay buffer (50 mM Bistris propane (pH 7.5), 50 mM KCl (omitted as appropriate), 10 mM $MgCl_2$, and 5 mM dithiothreitol). [C1-$^3H_1$]FDP (25 μM) precursor was added to start the reaction, and assays incubated for 5 min at 30 °C and stopped with the addition of 150 μl of 0.1 M KOH, 0.2 M EDTA solution. Assays were extracted with 0.5 ml of hexane and an aliquot taken for scintillation analysis. Control assays using boiled enzymes were used to determine background radioactive counts. Assays were linear with time and amount of enzyme in all cases.

GDP Activity Assays—Quadruplicate 1-ml assays for purified recombinant MdFAS1 and AcTPS2 enzymes were set up in 20-ml glass scintillation vials using the buffer described above and 50 μM [C1-$^3H_1$]GDP. Assays were overlaid with 5 ml hexane incubated at 30 °C for 20 min then extracted with vigorous vortexing. The PsTPS2 assays were carried out using 300 nM enzyme and 50 μM [C1-$^3H_1$]GDP in a previously described PsTPS2 monoterpene synthase buffer (44).

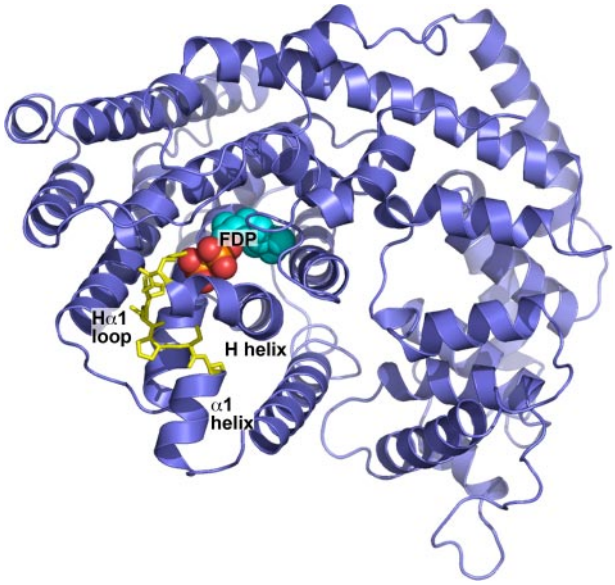

FIGURE 1. **Homology model for the apple α-farnesene synthase MdAFS1.** The model was constructed using Modeler9 version 1 by threading the MdAFS1 sequence into the three-dimensional coordinates of bornyldiphosphate synthase structure (PDB accession 1N20) and energy minimizing. The H-α1 loop region (*yellow*) is shown in stick representation. FDP substrate, as determined by GOLD docking analysis, is also indicated.

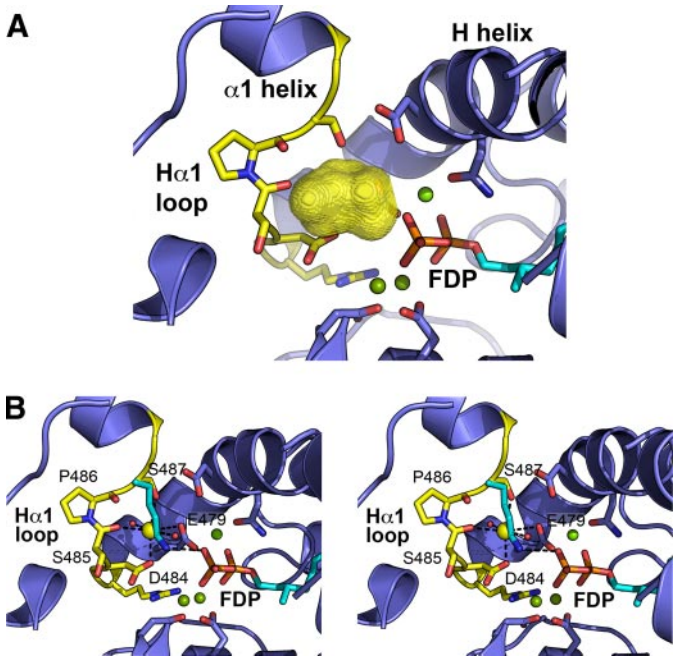

FIGURE 2. **Proposed potassium binding cavity in MdAFS1.** *A*, the H-α1 loop region largely defines the boundary of an approximate 200 Å^3 cavity (represented by the three-dimensional *yellow* surface). Selected residues (*blue*) within the DD*XX*D (lower) and H helix NSE/DTE motifs with their associated bound magnesium atoms (*green*) and the diphosphate moiety of the FDP precursor are also shown. Positioning of magnesium atoms in the MdFAS1 homology model are based on the equivalent atoms in the BPPS crystal structure. *B*, stereoview plot showing proposed octahedral coordination of K^+ in MdAFS1 overlaid with the BPPS structure lysine residue (Lys^{512}), which is highly conserved in TPS-b enzymes. Three ligands are provided for by H-α1 loop residue atoms, namely the side chain carbonyl oxygens of Asp^{484} and Ser^{487} and main chain carbonyl oxygen of Ser^{485}. The octahedral arrangement is completed by two water molecules (*red*) and the side chain carbonyl oxygen atom of glutamate (Glu^{479}) residue. Glu^{479} forms part of the H helix NSE/DTE Mg^{2+} binding motif and hence is also likely to be involved in direct Mg^{2+} coordination. Positioning of K^+ is based on fulfilling the average 2.8-Å distance requirement for K-O bonds (52) and constraining the coordination geometry to that most commonly observed in M^+ metal-dependent enzymes (20).

Volatile Analysis—Headspace volatile analysis was done according to previously reported methods (21), although the initial GC oven temperature for identification of AcTPS2 and PsTPS2 monoterpenes was lowered to 30 °C. Solvent extractions (20 ml) derived from 5-ml enzyme reactions (31) in the presence of FDP were dried ($MgSO_4$) and reduced in volume to 200 μl, under a stream of N_2, prior to GC-MS analysis. GC-MS analysis used an Agilent 6890N GC coupled to a Waters GCT time-of-flight mass spectrometer. Separations were carried out on a 20 m × 0.18-mm inner diameter × 0.18-μm film thickness DB-Wax (Agilent) column at a helium flow of 1 ml min^{-1} after a 1-μl, 1-min splitless injection at 220 °C. The oven temperature ramp was 35 °C for 1 min, 5 °C min^{-1} to 240 °C, and hold for 1 min. Authentic compound retention time standards used were *E*-β-farnesene (Givaudan, Switzerland), and *Z*,*E*- and *E*,*E*-α-farnesene obtained from "Granny Smith" apples (47, 48), and quantification was against hexadecane.

RESULTS

Homology Modeling Identifies H-α1 Loop as a Probable K^+ Binding Region—An MdAFS1 homology model was used to identify regions that might be associated with K^+ binding. The model was generated by threading the MdAFS1 amino acid sequence onto the three-dimensional structure of its closest structural homologue, a bornyldiphosphate synthase (BPPS) structure complexed with a GDP analogue (36). Template and target structures shared 39% identity and 58% similarity over residues 33–576 (MdAFS1 numbering), which correspond to the complete enzyme structure following the RRX_8W motif. Prior to this motif the polypeptide is typically disordered (49) and exhibits little amino acid homology between TPS enzymes.

The association of M^+ activation with divalent cations such as Mg^{2+}, taken together with the observation that M^+ binding sites frequently occur within surface-exposed loops (50), pointed to a potential K^+ binding region in MdAFS1. Several loop regions in TPS, including the A-*C*, H-α1, and J-K loops, are reported to be important for catalysis (33–36, 51). Of these, the MdAFS1 H-α1 loop (Arg^{483}-Ser^{488}) (Fig. 1) in particular exhibited many of the criteria expected in a K^+ binding region. This surface-exposed loop, which lies within 4–6 Å of the conserved Mg^{2+} binding DD*XX*D motif and the diphosphate moiety of the bound substrate, provides a number of backbone or side chain oxygen atoms that could fulfill the average 2.8-Å distance requirement for K-O bonding (52). The loop helps enclose a small cavity, ~200 Å^3 in volume (Fig. 2*A*), into which project potential K^+ ligands, including the side chains of Asp^{484} and Ser^{487}, together with the main chain carbonyl oxygen of Ser^{485}. The side chain oxygen of the H helix NSE/DTE Mg^{2+} binding glutamate (Glu^{479}) residue (51, 53) (Fig. 2*B*) provides another potential ligand.

Asp^{484} and Ser^{487} Residues Are Crucial for MdAFS1 Activity—To probe the role in K^+ binding of the H-α1 loop in MdAFS1, four mutations (D484A, S485A, S487A, and S488A) were constructed and the respective single-site mutant enzymes overexpressed in *Escherichia coli*. The role of Pro^{486} within the H-α1 loop was not probed by mutagenesis as it must confer some

rigidity to the MdAFS1 H-α1 loop and hence be important for its structural integrity.

The mutant enzymes were tested for their ability to convert [C1-$^3H_1$]FDP into solvent-extractable products, either in the presence or absence of 50 mM KCl (Fig. 3). They were also analyzed for GDP activity in the presence of KCl. Full activity comparisons between the MdAFS1 WT and H-α1 loop mutants in the presence of K^+ are summarized in Table 1.

Our results show an overall 95% decrease in sesquiterpene synthase activity in the S487A mutant and an 85% loss of activity in the D484A mutant compared with WT enzyme, when K^+ is present, with little change in K^+ independent activity. The S485A mutant exhibited marginally increased sesquiterpene synthase activities, and surprisingly an approximate 2-fold increase in monoterpene synthase activity compared with the WT enzyme (Table 1). This was confirmed semi-quantitatively using GC-MS (supplemental Fig. S1). The S488A mutant showed decreases in both sesqui- and mono-TPS activities, compared with the WT enzyme, with mono-TPS activity being reduced more than sesqui-TPS activity. GC-MS analysis also established that the mono-TPS ((*E*)-β-ocimene and β-myrcene) (supplemental Fig. S2) and sesqui-TPS (α-farnesene) products produced by the mutated and WT enzymes were identical and that there were no significant alterations in the ratios of the α-farnesene isomers produced (Table 2). The above observations highlight the importance of specific H-α1 loop residues in MdAFS1 enzyme function and offer intriguing clues to possible roles in M^+ coordination.

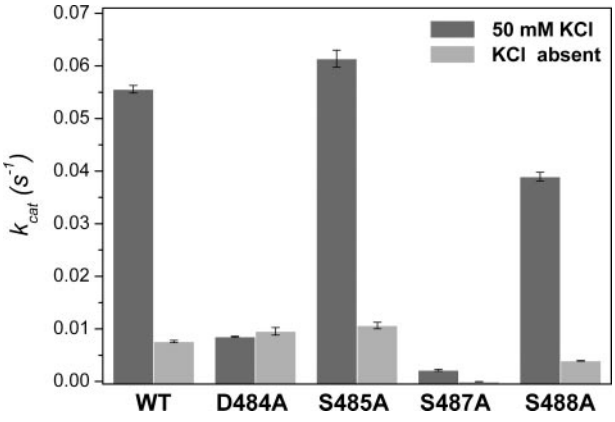

FIGURE 3. **Potassium responses for wild-type and H-α1 loop mutated MdAFS1.** Background subtracted scintillation activity data were obtained from hexane extractions of 50-μl assays containing 300 nM recombinant enzyme and 25 μM [C1-$^3H_1$]FDP, either in the presence or absence of 50 mM KCl. All experiments were carried out at least twice. Data are presented as mean ± S.E., $n = 4$.

To identify whether MdAFS1 behaved kinetically as a type I or type II enzyme a K^+ response curve was also generated for the WT enzyme (Fig. 4). This analysis showed that MdAFS1 exhibited a type II K^+ response (*i.e.* k_{cat} changes with [M^+] but does not reach zero when [M^+] = 0). It also re-affirmed the low millimolar (3–5 mM in this instance) k_a previously reported for K^+ in MdAFS1 (21).

Introduction of a Conserved Terpene Synthase Lysine Restores Activity Independent of K^+ in MdAFS1—Previous phylogenetic comparisons of MdAFS1 (21, 54) indicated that it clustered with the TPS-b synthases (Fig. 5*A*), a subgroup dominated by angiosperm mono-TPS enzymes that are not reported to have any M^+ dependence. A highly conserved H-α1 loop Lys residue was identified within the TPS-b subgroup members that utilized GDP as a substrate (Fig. 5*B*), suggesting that in these synthases this Lys side chain might provide a positive charge analogous to that of M^+ cations. The MdAFS1 residue corresponding to this Lys residue is Ser^{487}, already implicated by mutagenesis in K^+ binding (see above). To test the possible functional equivalence of these features within the TPS-b synthases, an additional MdAFS1 mutant (S487K) was constructed and the recombinant protein was tested for sesqui-TPS activity in the presence and absence of K^+.

The S487K mutant had 35–45% of the WT activity with FDP (Fig. 6), with no significant alterations in the α-farnesene isomer ratios produced (data not shown) and a small decrease in catalytic efficiency (WT and S487K respective k_{cat}/K_mvalues of 17.5 and 13.3 mM^{-1} s^{-1}) (supplemental materials Fig. S3 and Table S2 provide a more complete data profile of the S487K kinetics). More significantly, and in contrast to the WT enzyme, sesqui-TPS activity in S487K was independent of K^+, with the S487K activity approximately four times higher than the WT without K^+ (K_{cat} = 0.022 s^{-1} and 0.0062 s^{-1}, respectively). This finding provides clear evidence that the introduced Lys largely replaces the requirement for K^+, and hence strongly supports a role in M^+ coordination for Ser^{487} in MdAFS1. To our knowledge, this is the first report of a defined K^+ binding region in any TPS.

Mutagenesis of H-α1 Loop Residues in Other Terpene Synthases—The conservation of residues in the H-α1 loop region was also compared between MdAFS1 and enzymes of the TPS-d subgroup, which largely comprise K^+-dependent mono-TPS (Fig. 7). Interestingly, these sequence comparisons revealed a completely conserved Ser residue in the TPS-d subgroup, equivalent to Ser^{487} in MdAFS1. A Sitka spruce (*Picea sitchensis*) pinene synthase (PsTPS2) (44) was selected from this group for mutagenesis to establish whether its

TABLE 1

Terpene synthase activities for MdAFS1 (WT) and H-α1 loop mutants

Relative activity (V_{rel}) percentages are based on non-mutated (WT) MdAFS1. All k_{cat} s^{-1} values represent mean ± S.E., $n = 4$.

Enzyme	FDP activity, K_{cat} [a]	V_{rel}	GDP activity, K_{cat} [b]	V_{rel}	GDP/FDP
	s^{-1}	%	s^{-1}	%	
WT	0.0553 ± 0.0003	100	0.000281 ± 0.00001	100	0.51
D484A	0.0086 ± 0.0001	15	0.000034 ± 0.00002	12	0.40
S485A	0.0613 ± 0.0006	110	0.000588 ± 0.00002	209	0.96
S487A	0.0026 ± 0.0003	4.7	0.000005 ± 0.00001	1.8	0.20
S488A	0.0390 ± 0.0003	72	0.000052 ± 0.00002	18	0.13

[a] At 25 μM, [C1-$^3H_1$]FDP, 10 mM $MgCl_2$, 50 mM KCl.
[b] At 50 μM, [C1-$^3H_1$]GDP, 10 mM $MgCl_2$, 50 mM KCl.

TABLE 2

Farnesene isomer composition from WT and H-α1 loop MdAFS1 enzymes

Retention times (RT) and farnesene isomer percentages are given. Authentic standards used were (*E*)-β-farnesene, (*Z*,*E*)- and (*E*,*E*)-α−farnesene. (*E*,*Z*)- and (*Z*,*Z*)-α−farnesene and (*Z*)-β-farnesene were identified based on MS and relative retention times.

Compound	RT	WT	D484A	S485A	S488A
	min				
(*Z*)-β-Farnesene	16.95	25	NA[a]	27	NA
(*E*)-β-Farnesene	17.65	75	NA	73	NA
(*Z*,*Z*)-α-Farnesene	18.33	11	11	14	9
(*E*,*Z*)-α-Farnesene	18.84	29	32	31	22
(*Z*,*E*)-α-Farnesene	18.98	19	19	18	23
(*E*,*E*)-α-Farnesene	19.45	41	38	37	46

[a] NA, not applicable.

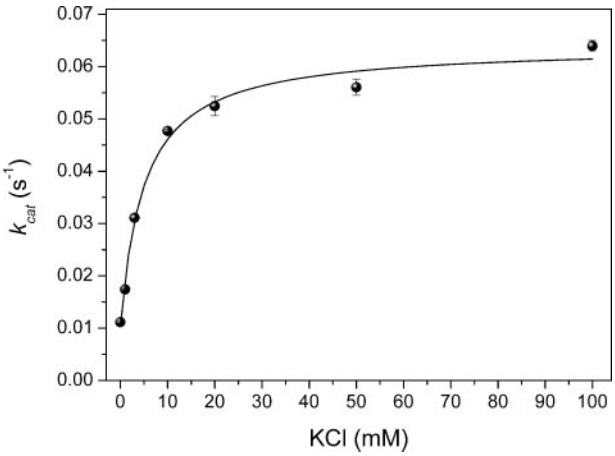

FIGURE 4. **Kinetic evaluation of MdAFS1 potassium dependence.** MdAFS1 exhibits a typical type II kinetic response to K^+ where activity is present when $[K^+] = 0$ and K_{cat} increases with $[K^+]$ to a finite value. Kinetic evaluation of K^+ was set up according to Green *et al.* (21) and experiments were carried out at least twice. Data are presented as mean ± S.E., $n = 4$.

H-α1 loop Ser (Ser^{538}) residue (Fig. 7) could also be implicated in K^+ binding. This was carried out by converting Ser^{538} in PsTPS2 to both Lys and Ala residues. In the reverse direction, an M^+ independent TPS-b kiwifruit (*Actinidia chinensis*) myrcene synthase (AcTPS2)[3] was selected to test the effect of converting the equivalent Lys (Lys^{514}) to Ala (Fig. 5*B*). Monoterpene synthase activities in the presence and absence of KCl for the resulting PsTPS2-S538A and AcTPS2-K514A mutant recombinant enzymes were compared with their WT counterparts (Fig. 8).

Our analysis confirmed the dependence of WT PsTPS2 on K^+ for activity and conversely, that WT AcTPS2 had no such reliance on this cation for proper function. In fact the WT AcTPS2 enzyme was significantly more active when KCl was absent from the activity buffer ($V_{rel} \sim 137\%$). Crucially our results also show that the PsTPS2-S538K mutant is not dependent on K^+ for mono-TPS activity (Fig. 8*A*). The almost identical activities observed for this mutant (k_{cat} 0.0112 s^{-1} and 0.0117 s^{-1}), whether K^+ was present or not, mirrored the previous findings in the equivalent MdFAS1 mutant. The activity observed when Ser^{538} in PsTPS2 was mutated to Lys equated to ~40% of the WT activity when K^+ was present, or an 8-fold increase over the WT enzyme when K^+ was absent. This again shows that the introduction of a Lys into the H-α1 loop of a K^+-dependent TPS can largely reverse the requirement for K^+. Notably, the importance of an equivalent Lys residue in AcTPS2 function was highlighted by the fact that when this Lys was mutated to Ala, in the K514A mutant of AcTPS2, a 90% reduction in its mono-TPS activity resulted (Fig. 8*B*).

The PsTPS2-S538A mutant resulted in an approximate 30% decrease in mono-TPS activity compared with the WT enzyme (*i.e.* k_{cat} 0.0202 s^{-1} compared with 0.0284 s^{-1}). Although the PsTPS2 mutation was less detrimental to its activity than the equivalent S487A mutation was to MdAFS1 activity (Table 1), this most likely reflects how well the remaining coordinating ligands in the two enzymes are still able to bind K^+.

GC-MS analysis confirmed that terpenes produced from the WT and mutant enzymes were identical, showing α- and β-pinenes from the two PsTPS2 mutants (supplemental Fig. 3) and low levels of β-myrcene from AcTPS2-K514A (supplemental Fig. S4).

An AcTPS2-K514S mutant was also generated and tested for activity in the presence and absence of K^+. This was done to see if a Ser introduced into the H-α1 loop of AcTPS2 could induce K^+ dependence. However, the presence of this Ser was not able to rescue any of the activity lost after the removal of the Lys residue (Fig. 8*B*).

The K^+ independent activity observed in both the MdAFS1 and PsTPS2 Ser → Lys mutants clearly demonstrates the importance of the H-α1 loop for provision of a positive charge in this region close to the active site, either through K^+ coordination or through a Lys residue. The similar involvement of this region in two functionally and phylogentically divergent TPS indicates it is also likely to be integral to the activity of other M^+-dependent TPS enzymes. The above analyses also highlight the requirement for the positive charge donated by the H-α1 loop Lys in the K^+-independent AcTPS2. Given the conservation of this Lys in TPS-b synthases, it is plausible and likely that its associated positive charge is also necessary for activity in the other K^+-independent monoterpene synthases.

DISCUSSION

The association of monovalent cations with enzymatic activity was first described by Boyer *et al.* (10) and in the intervening decades, detailed kinetic investigation has led to a wealth of knowledge regarding M^+ dependence. It has not been until the availability of high resolution crystal structures for M^+-activated enzymes, however, that a more complete picture, combining kinetic and mechanistic features, has materialized.

The dependence of terpene synthase activity on K^+ was first identified in TPS-d gymnosperm mono-TPS (44) and later established for a sesqui-TPS from apple (MdAFS1) (21). The TPS-d mono-TPS that include PsTPS2 have been reported to show an absolute dependence on K^+, whereas MdAFS1 still retains up to 12% of its activity in the absence of K^+ (Fig. 5). This residual activity cannot be accounted for by contamination from buffers or K^+ adventitiously bound to the *E. coli*-expressed enzyme, as we calculated this to account for less than 1% of the K^+ independent activity. Although these findings re-affirm that MdAFS1 is not absolutely dependent upon M^+ (21), its unequivocal classification as type I or type II K^+ acti-

[3] S. Green and N. J. Nieuwenhuizen, unpublished data.

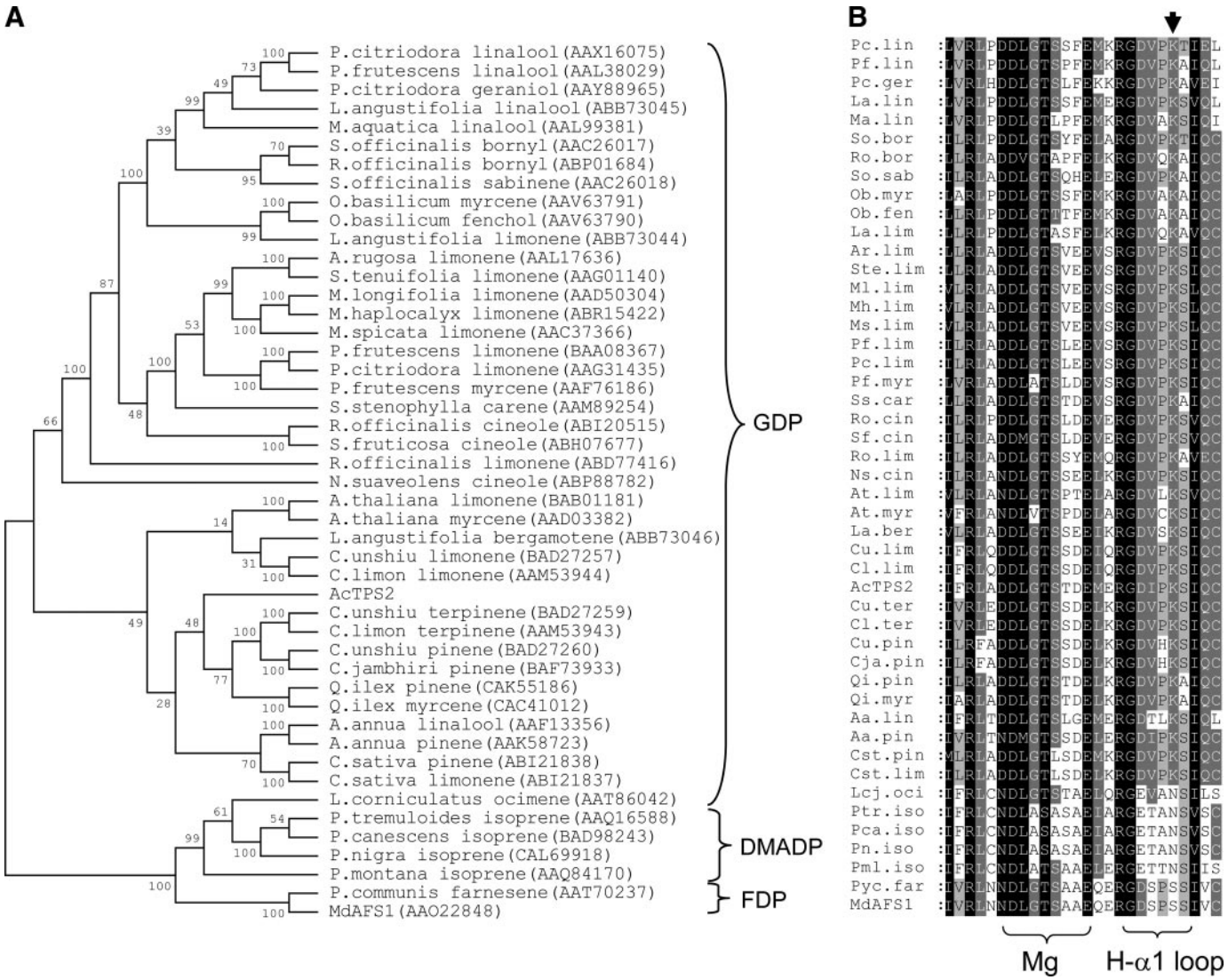

FIGURE 5. **Phylogentic and sequence analysis of TPS-b subgroup enzymes.** The unrooted Neighbor Joining (NJ) tree (*A*) indicates division of enzymes according to the production of monoterpenes (from GDP) and sesquiterpenes (from FDP) and isoprene from the 5-carbon dimethylallyl diphosphate (*DMADP*). The apple α-farnesene synthase and kiwifruit myrcene synthase are represented as MdAFS1 and AcTPS2, respectively. Bootstrap values and GenBank™ accessions are also given. *B* shows corresponding amino acid alignment of the approximate H-α1 loop and NSE/DTE magnesium binding regions in the TPS-b synthases and the conserved lysine (*down arrow*) equivalent to Ser^{487} in MdAFS1.

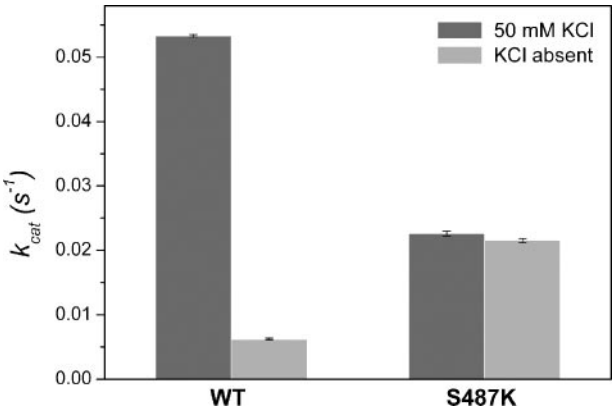

FIGURE 6. **Introduced H-α1 loop lysine effects on MdAFS1 potassium activation.** Sesquiterpene synthase activities for WT and S487K mutant MdAFS1 recombinant enzymes were derived from experiments using [C1-$^3H_1$]FDP in the same solvent extraction assay employed for the previous H-α1 loop mutants. Relative velocities (V_{rel}) of the WT and S487K mutants in the absence of KCl are also indicated and were calculated relative to their respective activities in the presence of KCl. Data are presented as mean ± S.E., $n = 4$.

vated, or that of any other TPS, will not be possible without high resolution structural data. This is due to the fact that type I enzymes can exhibit type II kinetics and vice versa (20).

In the absence of a crystal structure for a K^+-dependent TPS, homology modeling was used to identify regions within MdAFS1 that exhibited the potential for K^+ binding. This led to the identification of the surface-exposed H-α1 loop in MdAFS1 as one such region. This loop has been previously noted as functionally important in other TPS including BPPS, where it was shown that binding of the GDP diphosphate moiety triggers ordering of a number of polypeptide regions, including the H-α1 loop, which act to cap the active site pocket (36). This partitioning from the exterior solvent space prevents premature quenching of the highly reactive allylic carbocation intermediate.

Our observation of the importance of Ser^{487} in MdAFS1 K^+ binding now demonstrates a new role for the H-α1 loop in TPS catalysis. Mutagenesis also highlighted the relative importance

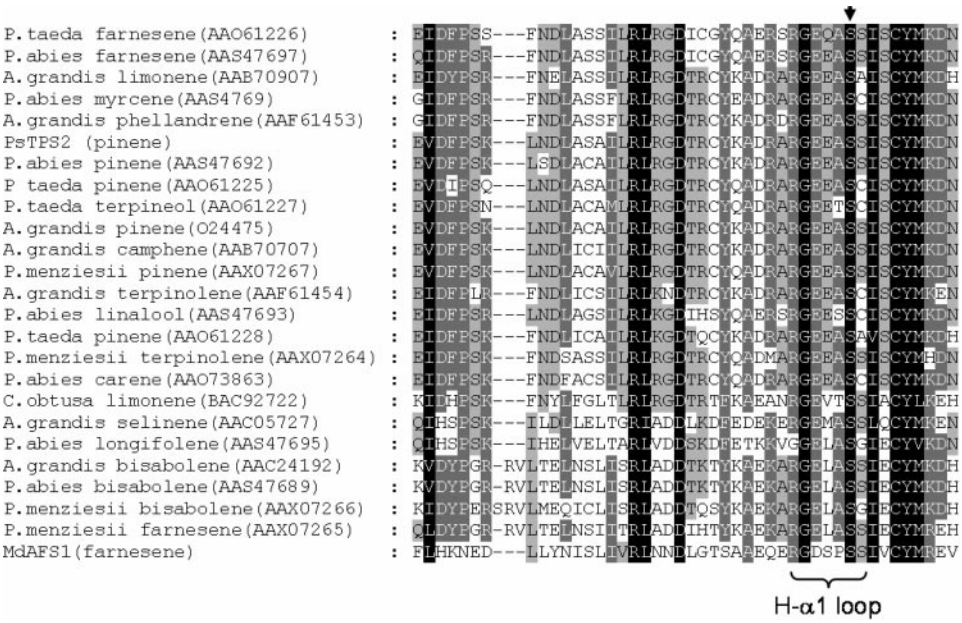

FIGURE 7. **TPS-d enzyme H-α1 loop region.** Amino acid alignment of the TPS-b subgroup and MdAFS1 enzymes illustrating the conserved H-α1 loop serine (down arrow) proposed to be involved in potassium binding. The Sitka Spruce pinene synthase (accession AAP72020) is denoted by its previously published PsTPS2 notation (44).

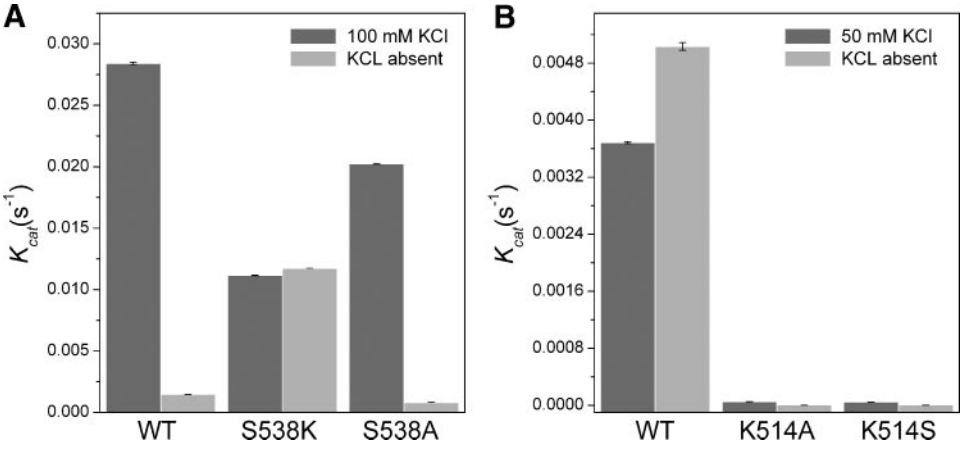

FIGURE 8. **Potassium responses for wild-type and H-α1 loop mutated PsTPS2 and AcTPS2 enzymes.** Activity data for PsTPS2 (*A*) and AcTPS2 (*B*) recombinant enzymes were obtained from hexane extractions of 1-ml assays containing 300 nM of each enzyme and 50 μM [C1-$^3H_1$]GDP, either in the presence or absence of KCl. Divalent metal ions used were 10 mM $MgCl_2$ for AcTPS2 and 10 mM $MnCl_2$ for PsTPS2 as specified by McKay *et al.* (44). All experiments were carried out at least twice and corrected for background precursor hydrolysis. Data are presented as mean $\pm$ S.E., $n = 4$.

the site (49). The H-α1 loop in K^+-dependent TPS enzymes appears to be another such example.

The large increase (~200%) in GDP activity and small (~10%) increase in FDP activity observed in the S485A mutant over the WT enzyme do not appear to be artifactual as replicated experiments exhibited a similar increase in both activities. The proximity of the H-α1 loop to the NSE/DTE sequence motif that forms a second Mg^{2+} binding site in TPS (51, 53) (residues 471–479 in MdAFS1) perhaps offers some insight into these observations. Substitution of Ser^{485} by Ala may free up space into which Arg^{482} could move, with some rearrangement of the backbone. This would bring the Arg^{482} guanidinium moiety closer to where Mg^{2+} would normally be bound in the MdAFS1 active site (supplemental Fig. S5). Consequently, the position of bound FDP or GDP may be altered in such a manner that provides more favorable interactions with active site aromatic residues implicated in carbocation stabilization (34) such as Tyr^{549} and Phe^{555} in MdAFS1, or basic residues (Arg^{289}) potentially poised for substrate PPi interaction (supplemental Fig. S5).

In addition to a probable role in capping the active site following substrate binding (34, 36), the MdAFS1 H-α1 loop, in tandem with K^+, appears to facilitate substrate binding. It does not, however, appear to have any direct role in determining product outcome, the terpenes produced from the WT and mutant MdAFS1 enzymes were essentially the same.

of other H-αl loop residues in MdAFS1 function with effects ranging from relatively minor (S488A) to significant changes (D484A and S485A) in activities while always maintaining product fidelity. The decrease in sesquiterpene synthase activity observed when Asp^{484} was converted to Ala, combined with favorable positioning of its side chain carboxyl oxygen (Fig. 2*B*), strongly points to its involvement as a second potential K^+ ligand. Further ligands are likely to be provided by the main chain carbonyl oxygen of Ser^{485} and the side chain carboxyl oxygen of Glu^{479}, which is located within the H helix NSE/DTE motif (Fig. 2*B*). Both groups are directed toward the putative K^+ binding site. It is frequently the case, however, that metal binding sites in proteins are formed by small loops in the polypeptide that provide a set of 3–4 ligands and thus define

The PsTPS2 mutagenesis, which focused on a conserved TPS-d Ser residue (equivalent to Ser^{487} in MAFS1), provided confirmatory evidence of the role of the H-α1 loop Ser^{487} in binding K^+. As with MdAFS1 analysis, this was demonstrated both by loss of activity when this Ser was mutated to Ala, and by the development of K^+ independent activity in the PsTPS2-S538K mutant (Fig. 8*A*). One notable difference between MdAFS1 and PsTPS2 was seen when their equivalent Ser residues were mutated to Ala. Although activity was almost completely abolished in the MdAFS1 S487A mutant (Table 1), ~70% of the PsTPS2 WT activity was retained in the S538A mutant (Fig. 8*A*). These activity effects are likely to relate to the ability of other ligands present in the two enzymes to contribute

to the coordination of K^+. Although these proposed ligands were not modeled in PsTPS2, a conserved TSPS-d glutamate residue (Glu^{535} in PsTPS2), three residues prior to the conserved serine, would be one obvious candidate. Mutagenesis of the equivalent Asp^{484} residue in MdAFS1 to Ala resulted in 85% reduction in activity (Table 1). Given the dependence of TPS-d synthases on K^+, the diphosphate moiety of GDP could potentially provide a third ligand. However, as with MdAFS1, confirmation of this and hence the correct classification of PsTPS2 as a type I or type II K^+-activated enzyme remains to be established.

The H-α1 loop in the TPS-b K^+-independent mono-TPS also appears to supply crucial positive charge by an alternative mechanism, involving the side chain of a conserved Lys. The almost complete loss of activity following its removal in AcTPS2 (Fig. 8*B*), combined with the capacity of the S487K and S538K mutations to confer K^+ independent activity upon MdAFS1 (Fig. 5) and PsTPS2 (Fig. 8*A*), respectively, is evidence of this. The H-α1 loop lysine residue (Lys^{512}) is observed to be hydrogen bonded to the PP_i anion in the BPPS crystal structure (Fig. 2*B*), and the ϵ-amino group of an equivalent Lys in a limonene synthase structure is similarly positioned (32). Although a definitive role for these H-α1 loop Lys residues remains unclear, the interaction with PP_i in BPPS suggests that it may be important for proper substrate binding. We infer that similar interactions are also possible in MdAFS1 and PsTPS2, this time utilizing a K^+ ion that makes either direct or indirect contact with PP_i. The conservation of Lys in the K^+-independent TPS-b enzymes also provides a structural explanation for the bifurcation of K^+ dependence within this subgroup.

A definitive resolution of the position of K^+ in both MdAFS1 and PsTPS2, and the additional coordinating atoms, will ultimately depend upon the availability of a high resolution crystal structures. Despite this, our proposed model for K^+ coordination in MdAFS1 (Fig. 2*B*) is strongly supported by the biochemical analysis of specific H-α1 loop residue mutants. When considering that 6 ligands in octahedral configuration is the most commonly observed geometry for M^+ coordination (20) it is likely that at least one and possibly two water molecules will prove to be involved in the completion of the K^+ coordination in MdAFS1. Although our model precludes a direct interaction between K^+ and substrate PP_i in MdAFS1 this cannot be completely ruled out especially when considering the inherent flexibility of protein loop regions and the apparent fluidity in the kinetics of enzymatic K^+ activation. Regardless of the exact architectural nature of this region it is likely that the positive charge donated by K^+ in the K^+-dependent TPS and the conserved H-α1 loop Lys in the K^+-independent TPS-b enzymes both act to help stabilize the H-α1 loop region for optimal substrate binding.

In summary, we have identified a new role for the H-α1 loop in terpene synthase catalysis, and pointed to the importance of specific residues within this loop for K^+ coordination in both MdAFS1 and PsTPS2, and for the activity of a K^+-independent mono-TPS. This study not only provides a basis for future analysis of terpene synthase M^+ activation but also insight into the wider role of the H-α1 loop in TPS catalysis.

Acknowledgments—We thank Dr. Jorg Bohlmann and Karen Reid (Michael Smith Laboratories, University of British Columbia, Vancouver, Canada) for making available the Sitka spruce pinene synthase expression construct.

REFERENCES

1. Croteau, R., Kutchan, T., and Lewis, N. (2000) *Biochemistry and Molecular Biology of Plants*, American Society of Plant Physiology, New York
2. Dudareva, N., and Pichersky, E. (2000) *Plant Physiol.* **122,** 627–634
3. Langenheim, J. H. (1994) *J. Chem. Ecol.* **20,** 1223–1280
4. Pare, P. W., and Tumlinson, J. H. (1999) *Plant Physiol.* **121,** 325–332
5. Takabayashi, J., and Dicke, M. (1996) *Trends Plant Sci.* **1,** 109–113
6. Pechous, S. W., Watkins, C. B., and Whitaker, B. D. (2005) *Postharvest Biol. Tech.* **35,** 125–132
7. Gapper, N. E., Bai, J., and Whitaker, B. D. (2006) *Postharvest Biol. Techn.* **41,** 225–233
8. Lesburg, C. A., Zhai, G., Cane, D. E., and Christianson, D. W. (1997) *Science* **277,** 1820–1824
9. Ashby, M., and Edwards, P. (1990) *J. Biol. Chem.* **265,** 13157–13164
10. Boyer, P. D., Lardy, H. A., and Phillips, P. H. (1942) *J. Biol. Chem.* **146,** 673–682
11. Mudd, S. H., and Cantoni, G. L. (1958) *J. Biol. Chem.* **231,** 481–492
12. O'Brien, M. C., and McKay, D. B. (1995) *J. Biol. Chem.* **270,** 2247–2250
13. Viitanen, P. V., Lubben, T. H., Reed, J., Goloubinoff, P., O'Keefe, D. P., and Lorimer, G. H. (1990) *Biochemistry* **29,** 5665–5671
14. Wu, Y., Qian, X., He, Y., Moya, I. A., and Luo, Y. (2005) *J. Biol. Chem.* **280,** 722–728
15. Cane, D. E. (1990) *Chem. Rev.* **90,** 1089–1103
16. Croteau, R. (1987) *Chem. Rev.* **87,** 929–954
17. Tholl, D. (2006) *Curr. Opin. Plant Biol.* **9,** 297–304
18. Evans, H. J., and Sorger, G. J. (1966) *Annu. Rev. Plant Physiol.* **17,** 47–76
19. Suelter, C. H. (1970) *Science* **168,** 789–795
20. Page, M. J., and Di Cera, E. (2006) *Physiol. Rev.* **86,** 1049–1092
21. Green, S., Friel, E. N., Matich, A., Beuning, L. L., Cooney, J. M., Rowan, D. D., and MacRae, E. (2007) *Phytochemistry* **68,** 176–188
22. Beilby, M. J., and Blatt, M. R. (1986) *Plant Physiol.* **82,** 417–422
23. Savage, T., Hatch, M., and Croteau, R. (1994) *J. Biol. Chem.* **269,** 4012–4020
24. Croteau, R., Gershenzon, J., Wheeler, C. J., and Satterwhite, D. M. (1990) *Arch. Biochem. Biophys.* **277,** 374–381
25. Croteau, R., Satterwhite, D., Cane, D., and Chang, C. (1988) *J. Biol. Chem.* **263,** 10063–10071
26. Croteau, R., Satterwhite, D., Wheeler, C., and Felton, N. (1989) *J. Biol. Chem.* **264,** 2075–2080
27. Croteau, R., and Satterwhite, D. M. (1989) *J. Biol. Chem.* **264,** 15309–15315
28. Dueber, M. T., Adolf, W., and West, C. A. (1978) *Plant Physiol.* **62,** 598–603
29. Frost, R. G., and West, C. A. (1977) *Plant Physiol.* **59,** 22–29
30. Robinson, D. R., and West, C. A. (1970) *Biochemistry* **9,** 80–89
31. Caruthers, J. M., Kang, I., Rynkiewicz, M. J., Cane, D. E., and Christianson, D. W. (2000) *J. Biol. Chem.* **275,** 25533–25539
32. Hyatt, D. C., Youn, B., Zhao, Y., Santhamma, B., Coates, R. M., Croteau, R. B., and Kang, C. (2007) *Proc. Natl. Acad. Sci. U. S. A.* **104,** 5360–5365
33. Rynkiewicz, M. J., Cane, D. E., and Christianson, D. W. (2002) *Biochemistry* **41,** 1732–1741
34. Shishova, E. Y., DiCostanzo, L., Cane, D. E., and Christianson, D. W. (2007) *Biochemistry* **46,** 1941–1951
35. Starks, C. M., Back, K., Chappell, J., and Noel, J. P. (1997) *Science* **277,** 1815–1820
36. Whittington, D. A., Wise, M. L., Urbansky, M., Coates, R. M., Croteau, R. B., and Christianson, D. W. (2002) *Proc. Natl. Acad. Sci. U. S. A.* **99,** 15375–15380
37. Pechous, S. W., and Whitaker, B. D. (2004) *Planta* **219,** 84
38. Thompson, J. D., Gibson, T. J., Plewniak, F., Jeanmougin, F., and Higgins, D. G. (1997) *Nucleic Acids Res.* **25,** 4876–4882

39. Saitou, N., and Nei, M. (1987) *Mol. Biol. Evol.* **4,** 406–425
40. Zuckerkandl, E., and Pauling, L. (1965) *Evolutionary Divergence and Convergence in Proteins*, Academic Press, New York
41. Tamura, K., Dudley, J., Nei, M., and Kumar, S. (2007) *Mol. Biol. Evol.* **24,** 1596–1599
42. Marti-Renom, M. A., Stuart, A. C., Fiser, A., Sanchez, R., Melo, F., and Sali, A. (2000) *Annu. Rev. Biophys. Biomol. Struct.* **29,** 291–325
43. Jones, G., Willett, P., and Glen, R. C. (1995) *J. Mol. Biol.* **245,** 43–53
44. McKay, S. A., Hunter, W. L., Godard, K.-A., Wang, S. X., Martin, D. M., Bohlmann, J., and Plant, A. L. (2003) *Plant Physiol.* **133,** 368–378
45. Studier, F. W. (2005) *Protein Expression Purif.* **41,** 207–234
46. Greenhagen, B. T., O'Maille, P. E., Noel, J. P., and Chappell, J. (2006) *Proc. Natl. Acad. Sci. U. S. A.* **103,** 9826–9831
47. Murray, K. E. (1969) *Aust. J. Chem.* **22,** 197–204
48. Anet, E. (1970) *Aust. J. Chem.* **23,** 2101–2108
49. Williams, D. C., McGarvey, D. J., Katahira, E. J., and Croteau, R. (1998) *Biochemistry* **37,** 12213–12220
50. Harding, M. (2004) *Acta Crystallogr. Sect. D Biol. Crystallogr.* **60,** 849–859
51. Rynkiewicz, M. J., Cane, D. E., and Christianson, D. W. (2001) *Proc. Natl. Acad. Sci. U. S. A.* **98,** 13543–13548
52. Harding, M. (2002) *Acta Crystallogr. Sect. D Biol. Crystallogr.* **58,** 872–874
53. Cane, D. E., and Kang, I. (2000) *Arch. Biochem. Biophys.* **376,** 354–364
54. Martin, D. M., Faldt, J., and Bohlmann, J. (2004) *Plant Physiol.* **135,** 1908–1927